

## **Felsic Xenoliths in Corundum-related Basalt at Khao Lun Tom, Bo Phloi District, Kanchanaburi Province, Western Thailand**

Chakkaphan Sutthirat<sup>1,2\*</sup>, Yanticha Namphet<sup>1</sup> and Nuttee Shitangkool<sup>1</sup>

<sup>1</sup> Department of Geology, Faculty of Science, Chulalongkorn University, Bangkok 10330 Thailand

<sup>2</sup> The Gem and Jewelry Institute of Thailand (Public Organization), Faculty of Science, Chulalongkorn University, Bangkok 10330 Thailand

\*Corresponding author: c.sutthirat@gmail.com and chakkaphan.s@chula.ac.th

Received 16 July 2010 Accepted 23 August 2010

### **Abstract**

Felsic xenoliths found within an area of Cenozoic alkali basalt related to corundum deposit in Bo Phloi district, Kanchanaburi province, western Thailand, were collected for this study. Petrography, mineral chemistry and whole-rock geochemistry were carried out and aimed to find relationship with corundum formation. Based on petrographic description, alkali feldspar, plagioclase and quartz are significantly essential minerals whereas accessory minerals are composed of biotite, zircon, apatite and ilmenite. Porphyritic and poikilitic textures are clearly distinguished as primary texture, particularly in feldspar grains; besides, quenched texture and reaction product induced by basaltic magma usually present around edges of these feldspars. Whole-rock geochemistry also yields similar result with slight variation in composition. These xenoliths can be classified, based on petrochemical data, as granite to syenite. Alumina saturations of all xenolith samples are classed as peraluminous series which normative corundum present sometimes in these samples. Essential minerals of these felsic xenoliths have similar chemical compositions. Feldspar compositions, in particular, are equivalent to about 700-800°C of equilibrated temperature, estimated at a pressure of 5 Kbar, and they seem to have been heated up to over 1000°C by basaltic magma. In conclusion, these felsic xenoliths appear to have originated in high aluminous igneous provenances in which differentiation processes had been taken place before picking up and transportation to the surface via basaltic eruption. Although, corundum has potential to crystallize within some of these xenoliths, corundum crystal has never been found during this study. However, more samples should be collected for further investigation.

**Keywords:** basalt, corundum, petrochemistry, Thailand, xenolith

### **1. Introduction**

Bo Phloi basalt, located in Kanchanaburi province about 150 km west of Bangkok, still remains as a volcanic plug overspreading a small area of about 500 m<sup>2</sup> where is mostly covered by brownish residual soils. It has been defined as gem-related rock which has close relationship with deposits of corundum (mainly blue and yellow sapphires), black spinel, black pyroxene and other associated minerals. These deposits are mainly characterized by fluvial and terrace sediments forming along about N-S trending structure parallel to the Silurian-Devonian basement (Fig. 1). Petrochemistry of basalt was

investigated and classified as basanitoid and nepheline hawaiite (Barr and Macdonald, 1981). Its age was reported as 4.17±0.11 Ma using <sup>40</sup>Ar/<sup>39</sup>Ar age-dating technique (Sutthirat *et al.*, 1994) and 3.14±0.17 Ma using K/Ar age-dating technique (Barr and Macdonald, 1981). This Late Cenozoic alkali basalt was a part of enormous volcanism in mainland Southeast Asia which had been erupted as a consequence of extensional heating after continental collision between Indian plate and southern margin of the Eurasian continent (McCabe *et al.*, 1988; Tapponnier *et al.*, 1982). In addition, basalt contains varieties of xenolith

and xenocryst that appear to have been picked up from the deep seated provenance. Corundum and associated minerals may have been formed earlier in some particular formation beneath the earth surface prior to being transported by basaltic lava. Ultramafic xenoliths, mainly spinel lherzolite, were initially investigated; consequently, these xenoliths have been suspected unlikely to have relationship with sapphire formation but they appear to have been originated with upper mantle (Sutthirat *et al.*, 1999; Srithai, 2005). However, initial origin of sapphire was suspected to be related to felsic xenoliths (Sutthirat, 2001) or hybrid igneous rocks in the shallower crust (Guo *et al.*, 1994).

This study is, therefore, focused on felsic xenoliths associated with Bo Phloi basalt. These xenoliths were then collected for investigations of petrography, mineral chemistry and whole-rock geochemistry. Twenty three samples were prepared as thin sections for petrographic description under polarizing microscope. Subsequently, nine representative samples were picked up for polished-thin sectioning and analysis of mineral chemistry using an Electron Probe Micro-Analyzer (EPMA) model JEOL JXA-8100. Analytical conditions were set at 15 kV and about 2  $\mu$ A using a focused beam ( $<1 \mu\text{m}$  in diameter); mineral and pure oxide standards were used for calibration at the same condition prior to automatic ZAF correction and reporting of weight percent oxides. Rock-powdering was carried out for whole-rock geochemistry using a X-ray Fluorescence Spectrometer (XRFs), Bruker model AXS S-4 Pioneer. Press powder technique was applied with analytical condition of maximum rating  $\leq 4$  kV, 50 Hz and 8 kVA before calibration of internal standards and reporting of weight percent oxides. All research facilities are based at Faculty of Science, Chulalongkorn University.

## 2. Felsic Xenoliths

All of felsic xenolith samples were collected from fresh basalt and also weathered topsoil.

They have various sizes ranging from 3 to 30 cm in diameter and usually show moderately to highly weathered surfaces. Their colors are slightly different due to intensity of basaltic reaction and degree of subsequent weathering (Fig. 2a, c and e). In general, they are usually characterized by porphyritic texture with feldspar phenocrysts ranging from 0.5 to 2 cm (Fig. 2a and c). However, equigranular medium- to coarse-grained rocks have also been found (Fig. 2e). Moreover, a few nodules show foliated feature (Fig. 2a and c). Mineral assemblages, identified under polarizing microscope, usually comprise allotriomorphic holocrystalline crystals of quartz, alkali feldspar and plagioclase which their sizes range from 0.2 to 2 mm (Fig 2b, d and f). Alkali feldspar and plagioclase usually form as phenocrysts bigger than 2 mm in size. Biotite, apatite, opaque minerals and zircon were grouped as accessory assemblages. Poikilitic textures were also observed as primary texture, particular in big feldspar phenocrysts. Quenched texture and reaction materials were always found around feldspar grains in all nodules (Fig. 2b, d and f). All samples have similar assemblages and textures as reported above; however, the main assemblages are slightly different and ranging from 35-45% plagioclase, 25-30% alkali feldspar and 15-20% quartz. All accessory minerals, e.g., biotite, zircon, apatite and opaque mineral, may make up to 10%. Opaque minerals were identified, based on EPMA data as ilmenite and iron sulfide. Calcite was also accidentally discovered during EPMA analysis in a few samples. In addition, orthopyroxene, clinopyroxene, sphene and uncommon apophyllite (consisting of Si-Ca-K with some other elements) were rarely found in quartz-absent felsic xenoliths by Sutthirat (2001).

Based on these petrographic data, felsic xenoliths appear to have associated within felsic igneous provenance with lower quartz content that may have undertaken various degree of partial melting or differentiation processes yielding slightly different assemblages. These rocks were later picked up and partially modified by basaltic magma during rising up to the surface.

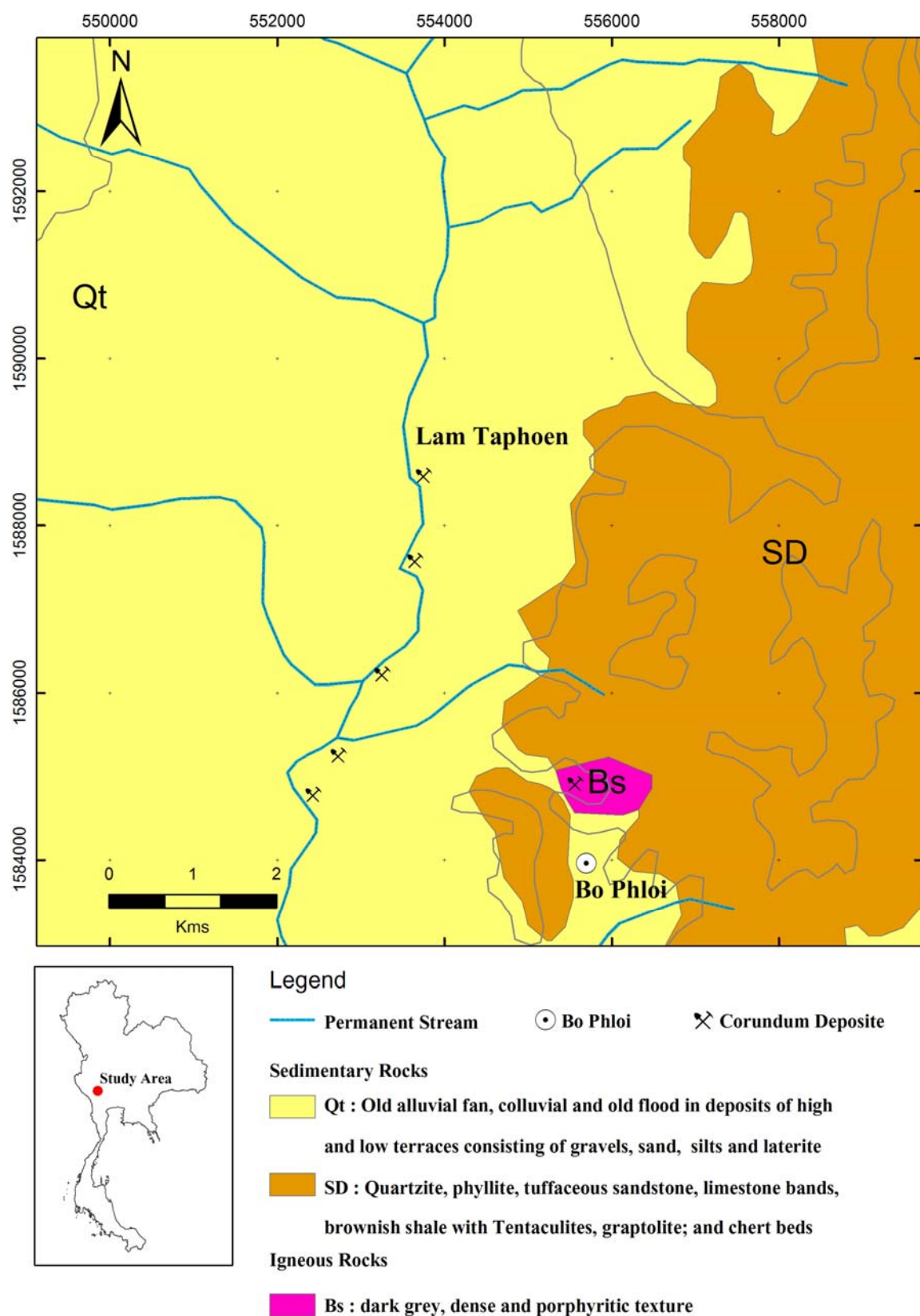


**Figure. 1** Geologic map of Bo Phloi area showing sediment and rock formations and location of the study area within a basaltic exposure (modified after DMR, 1976).

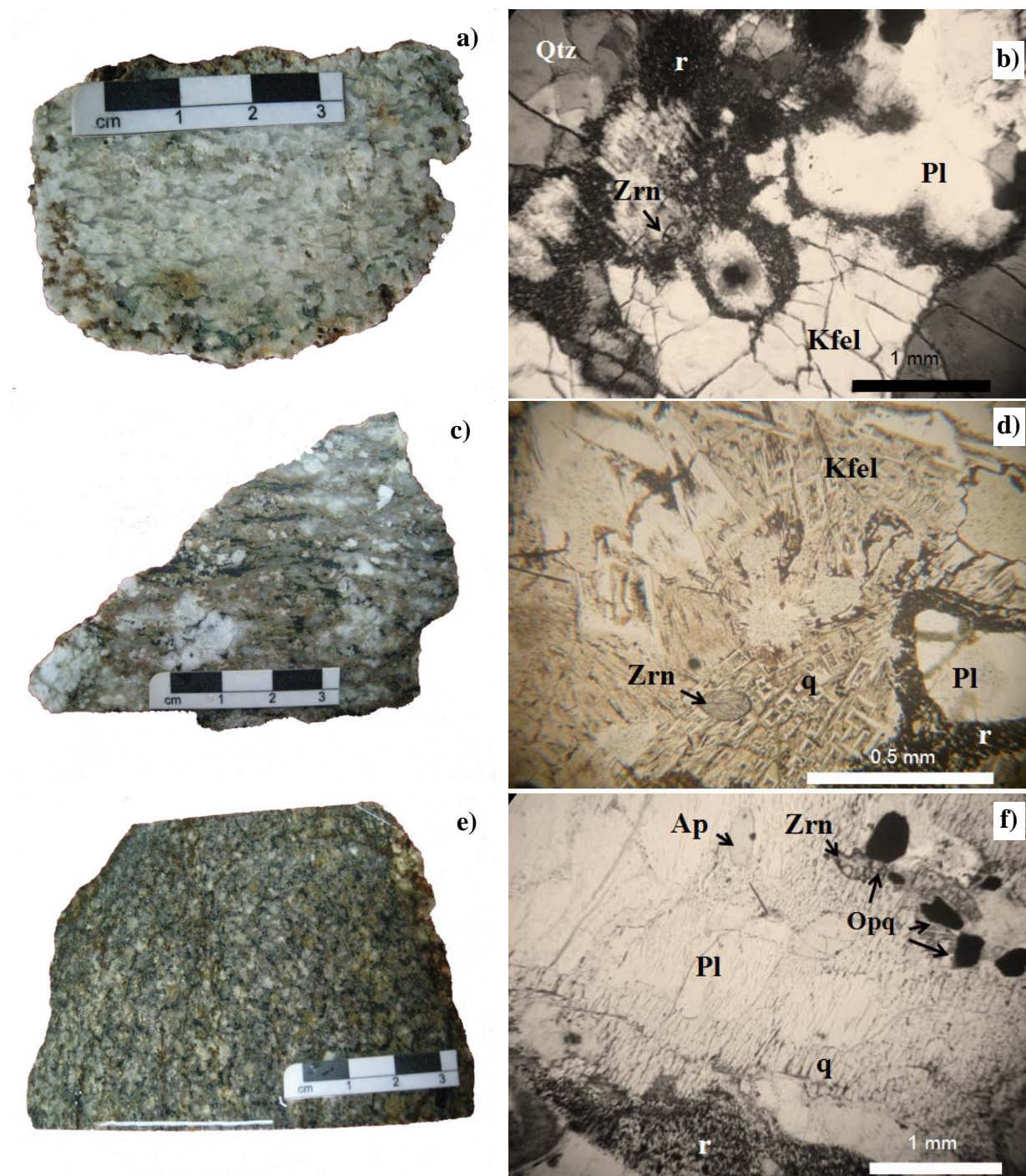


**Figure 2.** Felsic xenolith samples collected from Bo Phloi basalt, Kanchanaburi Province, Western Thailand. Figs 2a, c and e show representative hand specimens with phaneritic porphyritic texture and foliated feature in some nodules (a and c) and rare equigranular nodule with darker tone (e). Figs 2b, d and f are photomicrographs (PPL) of equivalent specimens on left column showing main assemblage of alkali feldspar (Kfel), plagioclase (Pl) and quartz (Qtz) with accessories of zircon (Zrn), apatite (Ap) and opaque mineral (Opq). Secondary features are clearly observed, particularly quenched texture (q), dark aggregated materials (r) of reaction.

### 3. Whole-Rock Geochemistry

Whole-rock major and minor analyses are summarized and presented in Table 1. In general, they vary within a narrow range. Their silica saturations fall between intermediate range (52–66%  $\text{SiO}_2$ ) and acidic range (>66%  $\text{SiO}_2$ ) whereas alumina saturations are conclusively peraluminous range ( $\text{Al}_2\text{O}_3 > \text{Na}_2\text{O} + \text{K}_2\text{O} + \text{CaO}$ ). CIPW normative was also carried out and shown in the same table. Normative albite and orthoclase are significantly present in all samples whereas some nodules are absent in normative quartz. Normative pyroxene, both hypersthene and diopside, present in most samples. In addition, it is the most interesting to find normative corundum in some nodules.

Harker variation diagrams plotting of silica contents versus other oxides and magnesium numbers ( $\text{Mg}^{\#} = \text{MgO}/(\text{MgO} + \text{Fe}_2\text{O}_3_{\text{total}})$ ) against major oxides were investigated and selected as present in Fig. 3. Diagrams generally show scattering plots; however, some tends can be

observed such as increasing silica against decreasing of  $\text{MgO}$ ,  $\text{Fe}_2\text{O}_3$ ,  $\text{Al}_2\text{O}_3$ ,  $\text{Na}_2\text{O}$  and  $\text{K}_2\text{O}$ . For increasing of  $\text{Mg}^{\#}$ , most major oxides, except silica, appear to increase accordingly. TAS classification diagram (Cox *et al.*, 1979 later modified by Wilson, 1989) were applied for nomenclature of these felsic xenoliths (Fig. 4); consequently, syenite and granite are the most suitable names which are compatible to petrographic description.

In conclusion, these felsic xenoliths seem to have been related to peraluminous igneous provenance in which has potential to have corundum crystallization. However, geochemical variations of these rocks have been recognized within a narrow range that may be resulted by different compositions of initial rock layers. Corundum and their associated minerals may have occurred in some particular layers which were picked up and transported to the surface via basaltic eruption.

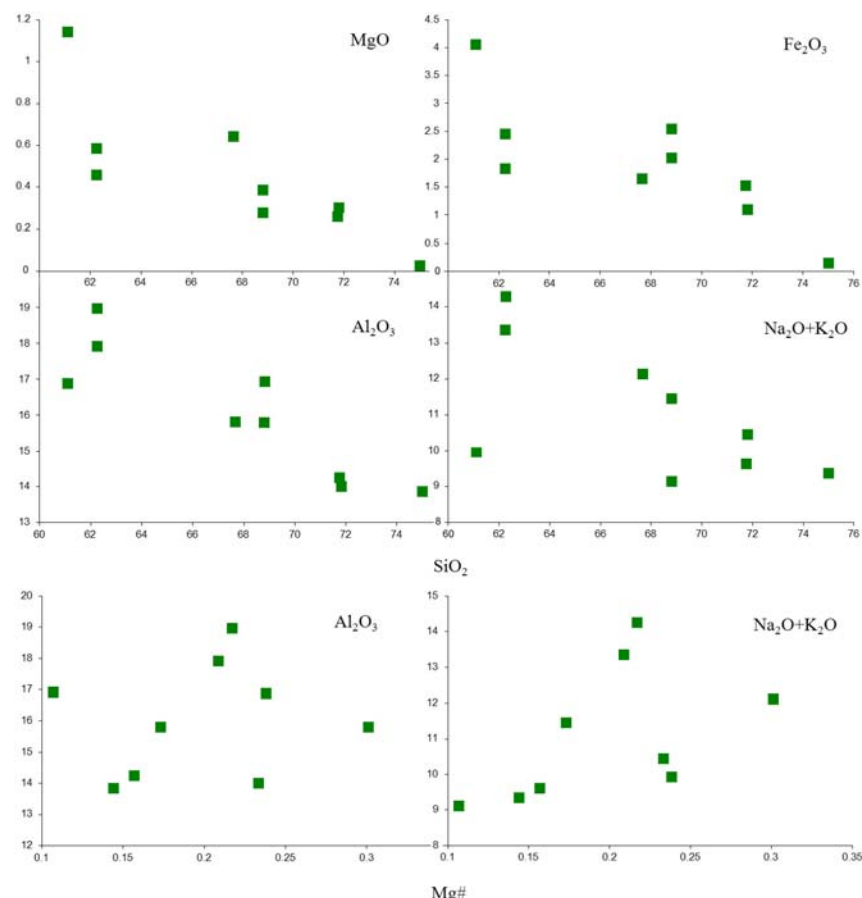


**Figure 3.** Selected variation diagrams plotting silica and magnesium number against major and minor compositions of felsic xenoliths samples.

**Table 1.** Major and minor chemical compositions analyzed using XRF technique and recalculated normative minerals of felsic xenolith samples from Bo Phloi basalt.

|                                | BP_2       | BP_4       | BP_5       | BP_6       | BP_7       | BP_12      | BP_21      | BP_23      | BP_24      |
|--------------------------------|------------|------------|------------|------------|------------|------------|------------|------------|------------|
| SiO <sub>2</sub>               | 71.76      | 68.82      | 75.02      | 62.27      | 61.11      | 71.83      | 62.26      | 67.67      | 68.83      |
| TiO <sub>2</sub>               | 0.29       | 0.45       | 0.08       | 0.24       | 1.56       | 0.26       | 0.68       | 0.38       | 0.55       |
| Al <sub>2</sub> O <sub>3</sub> | 14.23      | 15.79      | 13.84      | 18.96      | 16.88      | 13.99      | 17.9       | 15.8       | 16.92      |
| Fe <sub>2</sub> O <sub>3</sub> | 1.52       | 2.01       | 0.15       | 1.82       | 4.05       | 1.09       | 2.45       | 1.64       | 2.54       |
| MnO                            | 0.01       | 0.02       | nd         | 0.02       | 0.03       | 0.02       | 0.07       | 0.01       | 0.02       |
| MgO                            | 0.26       | 0.38       | 0.02       | 0.45       | 1.14       | 0.3        | 0.58       | 0.64       | 0.27       |
| CaO                            | 1.91       | 0.42       | 1.08       | 1.76       | 3.81       | 1.64       | 1.74       | 1.31       | 1.27       |
| K <sub>2</sub> O               | 6.51       | 7.73       | 6.36       | 11.62      | 5.37       | 7.42       | 8.61       | 7.71       | 7.92       |
| Na <sub>2</sub> O              | 3.09       | 3.71       | 2.97       | 2.63       | 4.55       | 3.02       | 4.73       | 4.39       | 1.19       |
| P <sub>2</sub> O <sub>5</sub>  | 0.11       | 0.36       | 0.11       | 0.03       | 0.97       | 0.06       | 0.33       | 0.07       | 0.26       |
| Total                          | 99.69      | 99.7       | 99.63      | 99.81      | 99.47      | 99.61      | 99.35      | 99.63      | 99.77      |
| CIPW Norm                      |            |            |            |            |            |            |            |            |            |
| Ap                             | 0.3        | 0.9        | 0.3        | 0.1        | 2.3        | 0.1        | 0.8        | 0.2        | 0.6        |
| Il                             | 0.6        | 0.9        | 0.1        | 0.5        | 3.0        | 0.5        | 1.3        | 0.7        | 1.1        |
| Or                             | 38.4       | 45.7       | 37.6       | 68.7       | 31.7       | 43.9       | 50.9       | 45.6       | 46.8       |
| Ab                             | 26.2       | 31.4       | 25.1       | 18.4       | 38.5       | 25.5       | 36.5       | 37.1       | 10.1       |
| An                             | 5.7        | 0.0        | 4.7        | 5.6        | 9.8        | 2.7        | 2.2        | 0.6        | 4.6        |
| <i>Crn</i>                     | <b>0.0</b> | <b>1.4</b> | <b>0.4</b> | <b>0.0</b> | <b>0.0</b> | <b>0.0</b> | <b>0.0</b> | <b>0.0</b> | <b>4.7</b> |
| Mag                            | 0.2        | 0.3        | 0.0        | 0.3        | 0.6        | 0.2        | 0.4        | 0.2        | 0.4        |
| Hem                            | 0.0        | 0.0        | 0.0        | 0.0        | 0.0        | 0.0        | 0.0        | 0.0        | 0.0        |
| Di                             | 2.6        | 0.0        | 0.0        | 2.5        | 2.4        | 4.1        | 3.6        | 4.5        | 0.0        |
| Hy                             | 1.2        | 3.4        | 0.2        | 0.0        | 5.5        | 0.0        | 0.0        | 1.3        | 3.8        |
| Wol                            | 0.0        | 0.0        | 0.0        | 0.0        | 0.0        | 0.1        | 0.0        | 0.0        | 0.0        |
| Qtz                            | 24.5       | 16.1       | 31.3       | 0.0        | 5.8        | 22.6       | 0.0        | 9.3        | 27.8       |
| Ol                             | 0.0        | 0.0        | 0.0        | 1.8        | 0.0        | 0.0        | 1.9        | 0.0        | 0.0        |
| Nep                            | 0.0        | 0.0        | 0.0        | 2.1        | 0.0        | 0.0        | 1.9        | 0.0        | 0.0        |

#### 4. Ternary Feldspar and Thermometry

Although, all minerals present in felsic xenolith samples were analyzed using EPMA for investigation of mineral chemistry, only feldspars, both plagioclase and alkali feldspar, were selected for further interpretation. The other minerals such as zircon, apatite, opaque minerals (iron sulfide and ilmenite) and calcite were identified and confirmed using their EPMA analyses. Feldspars, particularly alkali feldspar, are the most abundant minerals found in felsic nodules; besides, they can be used to estimate temperature of equilibration that may indicate part of the environment of rock provenance. Representative analyses of feldspars are

summarized in Table 2; in addition, ternary plots of end-member components were carried as shown in Fig. 5. Alkali feldspar show a wider compositional range ( $An_{2-10}Ab_{50-70}Or_{30-50}$ ) compared to those of plagioclase ( $An_{25-30}Ab_{55-65}Or_{5-15}$ ). This might be resulted by heat source of basaltic magma that yielded different degrees of alteration effecting alkali feldspar rather than plagioclase. Some compositions of alkali feldspar were shifted obviously from the common group whereas a few plagioclase compositions were slightly deviated from the main group (Fig. 5).

Ternary solvus isothermal lines estimated at a pressure of 5 Kbar using experimental data

of Elkins and Grove (1990) are added into ternary plots of feldspar (Fig. 5). Consequently, the compositions of coexisting ternary feldspars within the same nodules were tied together which mainly show constrain equilibration temperatures of about 700-800°C. Besides, a couple pairs appear to deviate up to 1000°C

which is equivalent to some unpaired compositions. This would imply alteration of feldspars' compositions induced by heating of basaltic magma during transportation prior to quenching onto the surface.

**Table 2.** Representative EPMA analyses of feldspars in felsic xenoliths from Bo Phloi basalt.

|                                | K-Feldspar |       |       |       |       |       |       | Plagioclase |       |       |       |       |       |       |
|--------------------------------|------------|-------|-------|-------|-------|-------|-------|-------------|-------|-------|-------|-------|-------|-------|
|                                | 4_1        | 4_2   | 5_1   | 5_2   | 6_1   | 6_2   | 7_1   | 7_2         | 2_1   | 2_2   | 4_1   | 4_2   | 5_1   | 5_2   |
| SiO <sub>2</sub>               | 65.91      | 65.92 | 64.54 | 65.35 | 66.18 | 64.77 | 65.16 | 64.92       | 60.80 | 60.47 | 60.02 | 59.50 | 59.67 | 59.40 |
| TiO <sub>2</sub>               | 0.03       | 0.00  | 0.63  | 0.00  | 0.00  | 0.00  | 0.08  | 0.04        | 0.00  | 0.02  | 0.02  | 0.04  | 0.04  | 0.03  |
| Al <sub>2</sub> O <sub>3</sub> | 19.38      | 19.54 | 19.86 | 20.27 | 19.47 | 22.40 | 20.63 | 20.88       | 24.08 | 25.05 | 24.66 | 25.33 | 25.66 | 25.73 |
| Cr <sub>2</sub> O <sub>3</sub> | 0.00       | 0.00  | 0.00  | 0.00  | 0.00  | 0.06  | 0.00  | 0.05        | 0.04  | 0.01  | 0.00  | 0.02  | 0.00  | 0.00  |
| Fe <sub>2</sub> O <sub>3</sub> | 0.03       | 0.06  | 0.49  | 0.06  | 0.00  | 0.10  | 0.14  | 0.11        | 0.28  | 0.06  | 0.05  | 0.07  | 0.00  | 0.07  |
| CaO                            | 0.49       | 0.46  | 1.02  | 0.54  | 0.35  | 0.41  | 1.73  | 1.85        | 5.43  | 5.62  | 6.24  | 6.57  | 6.15  | 6.51  |
| Na <sub>2</sub> O              | 5.83       | 5.60  | 5.45  | 6.16  | 6.08  | 7.88  | 7.09  | 7.08        | 6.68  | 7.45  | 6.59  | 7.04  | 7.43  | 7.31  |
| K <sub>2</sub> O               | 8.32       | 8.36  | 7.42  | 7.53  | 7.89  | 4.34  | 5.17  | 4.96        | 2.49  | 1.25  | 2.38  | 1.36  | 0.97  | 0.91  |
| Formula 8(O)                   |            |       |       |       |       |       |       |             |       |       |       |       |       |       |
| Si                             | 2.968      | 2.967 | 2.909 | 2.938 | 2.973 | 2.876 | 2.911 | 2.901       | 2.724 | 2.697 | 2.693 | 2.664 | 2.664 | 2.653 |
| Ti                             | 0.001      | 0.000 | 0.021 | 0.000 | 0.000 | 0.000 | 0.003 | 0.001       | 0.000 | 0.001 | 0.001 | 0.001 | 0.001 | 0.001 |
| Al                             | 1.029      | 1.036 | 1.055 | 1.074 | 1.031 | 1.173 | 1.086 | 1.099       | 1.271 | 1.316 | 1.304 | 1.336 | 1.350 | 1.354 |
| Cr                             | 0.000      | 0.000 | 0.000 | 0.000 | 0.000 | 0.002 | 0.000 | 0.002       | 0.001 | 0.000 | 0.000 | 0.001 | 0.000 | 0.000 |
| Fe <sup>3+</sup>               | 0.001      | 0.002 | 0.018 | 0.002 | 0.000 | 0.004 | 0.005 | 0.004       | 0.011 | 0.002 | 0.002 | 0.003 | 0.000 | 0.002 |
| Ca                             | 0.024      | 0.022 | 0.049 | 0.026 | 0.017 | 0.019 | 0.083 | 0.088       | 0.261 | 0.268 | 0.300 | 0.315 | 0.294 | 0.312 |
| Na                             | 0.509      | 0.489 | 0.476 | 0.537 | 0.529 | 0.679 | 0.614 | 0.613       | 0.580 | 0.644 | 0.573 | 0.611 | 0.643 | 0.633 |
| K                              | 0.478      | 0.480 | 0.427 | 0.432 | 0.452 | 0.246 | 0.295 | 0.283       | 0.142 | 0.071 | 0.136 | 0.078 | 0.055 | 0.052 |
| Total*                         | 5.010      | 4.997 | 4.955 | 5.008 | 5.002 | 4.998 | 4.996 | 4.991       | 4.990 | 5.000 | 5.008 | 5.009 | 5.008 | 5.007 |
| %End Members                   |            |       |       |       |       |       |       |             |       |       |       |       |       |       |
| %An                            | 2.3        | 2.2   | 5.2   | 2.6   | 1.7   | 2.0   | 8.3   | 9.0         | 26.5  | 27.3  | 29.7  | 31.4  | 29.6  | 31.3  |
| %Ab                            | 50.4       | 49.3  | 50.0  | 54.0  | 53.0  | 71.9  | 61.9  | 62.3        | 59.0  | 65.5  | 56.8  | 60.9  | 64.8  | 63.5  |
| %Or                            | 47.3       | 48.4  | 44.8  | 43.4  | 45.3  | 26.0  | 29.7  | 28.7        | 14.5  | 7.2   | 13.5  | 7.7   | 5.6   | 5.2   |

## 5. Discussions and Conclusions

Quenched texture and reaction materials observed in all felsic xenoliths were clearly resulted by interaction of basaltic magma from both direct chemical reaction and indirect processes of heating and quenching. These features have been clearly recognized under microscopic investigation; however, the alteration appears to have occurred along edges of feldspar grains that may indicate short period of interaction. Main initial compositions and textures of these xenoliths still remain in most samples. These felsic xenoliths can be classified, based on petrochemical data, as alkali granite to syenite. Although, their compositions may have

been modified by basaltic magma during transportation, they would be slightly changed and still indicate high alumina igneous provenance in which appear to have undertaken different degrees of partial melting and/or differentiation. Corundum has not yet been discovered in the xenoliths under microscopic investigation; however, normative corundum is present in a few nodules. This would be, at least, potential of corundum occurrence. More samples of felsic xenoliths should be collected for further study which may have more possibility to find corundum embedded within these rocks.

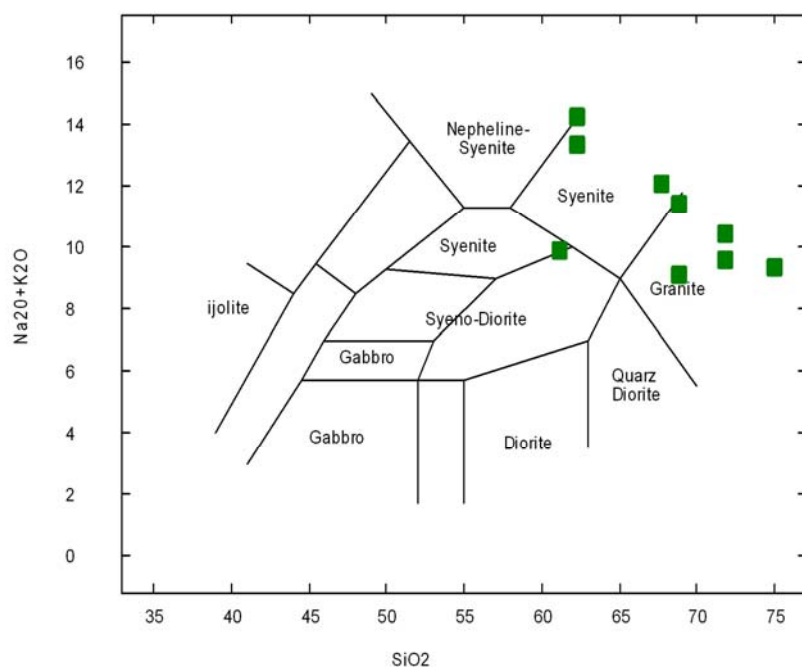


**Figure 4.** Chemical classification diagram (Cox *et al.*, 1979 modified by Wilson, 1989) plotting between  $\text{SiO}_2$  and  $\text{Na}_2\text{O}+\text{K}_2\text{O}$  contents of felsic xenoliths showing their compositions comparable to mainly granite and syenite. Variation of their composition shows alkali increasing towards decreasing trend of silica which seems to have good correlation.

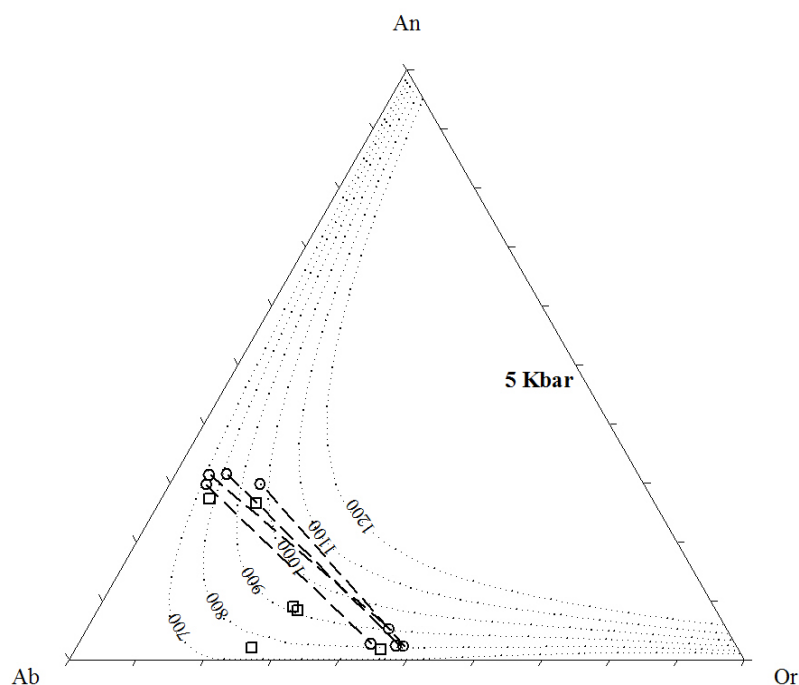


**Figure 5.** Ternary composition plots of feldspars found in xenolith samples. Isothermal solvus curves (dot lines) are calculated using database of Elkins and Grove (1990) at 5 Kbar. Dash tie lines connect between coexisting feldspars (circle plots) within the same xenoliths whereas square plots represent individual feldspars found in the other xenoliths.

However, the crucial evidence, corundum-sillimanite-zircon-spinel assemblage, named “*corsilzirspite*” was discovered accidentally within alluvial sapphire deposit and subsequently reported Pisutha-Arnond *et al.* (1998); it appears to have been formed by thermal metamorphism instead of igneous magmatism. Similar assemblage, sapphire-zircon-magnetite xenoliths, was also reported from Chanthaburi sapphire deposit, eastern Thailand prior to conclusion of an origin of felsic magma, such as phonolitic (nepheline syenite) magma, at the boundary between the crust and mantle. (Coenraads *et al.*, 1995). On the other hand, Guo *et al.* (1994) suggested a model of hybrid magmatism yielding sapphire and its associated minerals within basaltic terranes of eastern Asia and Australia. In addition, Sutherland *et al.* (1998) also suggested that corundum in basaltic fields may be formed by direct crystallization from silicate melt rather than metamorphic crystallization. Felsic xenoliths samples, granitic-syenitic rocks, under this study have composition as suggested by previous workers except *corsilzirspite* that may be part of contact metamorphism being form during partial melting of these felsic magmas. Based on tectonic model, enormous partial melting in the Western Thailand appear to have been taken place during a period of Late Cretaceous to Early Tertiary after Western Burma block collided into Shan Thai block resulting extensive granitic intrusions (both I type and S type) along this region including the study area (Charusiri *et al.*, 2002). Although corundum occurrence has never been discovered within this granitic belt corundum may have formed within enriched alumina granite-syenite situated in the deeper part.

## 6. Acknowledgements

This project was fully supported by the Gem and Jewelry Institute of Thailand (GIT) and Geology Department, Faculty of Science, Chulalongkorn University. The authors would like to thank Sopit Poompuang, Jiraprapa Neampan and Prachin Tongprachum for their generous support in laboratories and sample preparation. Adcharobon Laokhun and Atit Dornboonlon had been helping during the fieldwork.

## 7. References

Barr, S.M., and Macdonald, A.S. 1981. Geochemistry and geochronology of Late Cenozoic basalts of Southeast Asia. *Geological Society of America Bulletin*, 92(2): 1069-1142.

Charusiri, P., Ampaiwan, T., Hisada, K., Khaowiset, K., Kosuwan, S., and Daorerk, V. 2002. Geotectonic evolution of Thailand: Compilation and new synthesis. *Journal Scientific Research Chulalongkorn University (Section T)*, 1: 69-108.

Coenraads, R.R., Vichit, P., and Sutherland, F.L. 1995. An unusual sapphire-zircon-magnetite xenolith from the Chanthaburi Gem Province, Thailand. *Mineralogical Magazine*, 59: 465-479.

Cox, K.G., Bell, J.D., and Pankhurst, R.J. 1979. *The Interpretation of Igneous Rocks*. George, Allen and Unwin, London.

Department of Mineral Resources (DMR). 1976. Geological Map scale 1:250.000, Sheet ND 47-7.

Elkins, L.T., and Grove, T.L. 1990. Ternary feldspar experiments and thermodynamic models. *American Mineralogist*, 75: 544-559.

Guo, J., Griffin, W.L., and O'Reilly, S.Y. 1994. A cobalt-rich spinel inclusion in a sapphire from Bo Ploi, Thailand. *Mineralogical Magazine*, 58: 247-258.

McCabe, R., Celeya, M., Cole, J., Han, H.C., Ohnstadt, T., Paijitprapaporn, V., and Thitisawan, V. 1988. Extension tectonics: The Neogene opening of the N-S trend basin of central Thailand. *Journal of the Geophysical Researches*, 93: 11899-11910.

Pisutha-Arnold, V., Wathanakul, P., Intasopa, S., and Griffin, W.L. 1998. Corsilzirspite, a corundum sillimanite-zircon-hercynite rock: New evidence on the origin of Kanchanaburi sapphire, Thailand, *Proceedings of the Ninth Regional Congress on Geology, Mineral and Energy Resources of South East Asia GEOSEA 98*. Kuala Lumpur, 95-96 (Abstract).

Sutherland, F.L., Hoskin, P.W.O., Fanning, C.M., and Coenraads, R.R. 1998. Models of corundum origin from alkali basaltic



terrains: A reappraisal. *Contributions to Mineralogy and Petrology*, 133: 356-372.

Srithai, B. 2005. Petrography and mineral chemistry of ultramafic xenoliths from Bo Ploi basalt, Kanchanaburi, Thailand. *Proceedings of the International Conference on Geology, Geotechnology and MineralResource of Indochina*. Bangkok, 358-364.

Sutthirat, C. 2001. Petrogenesis of mantle and crustal xenoliths and xenocrysts in basaltic rocks associated with corundum deposits in Thailand. PhD Thesis (unpublished), Department of Earth Sciences, University of Manchester, UK, 445 pp.

Sutthirat, C. Charusiri, P., Farrar, E. and Clark, A.H. 1994. New  $^{40}\text{Ar}/^{39}\text{Ar}$  geochronology and characteristic of some Cenozoic basalt in Thailand. *Proceedings of the International Symposium on Stratigraphic Correlation of Southeast Asia*. Bangkok, 306-321.

Sutthirat, C., Droop, G.T.R., Henderson, C.M.B. and Manning D.A.C. 1999. Petrography and mineral chemistry of xenoliths and xenocrysts in Thai corundum-related basalts: Implications for the upper Mantle and lower crust beneath Thailand. *Proceedings of the Symposium on Mineral, Energy, and Water Resources of Thailand*. Bangkok, 152-161.

Tappognier, P., Peltzer, G., LeDain, A.Y., Armijo, R., and Cobbold, P. 1982. Propagating extrusion tectonics in Asia: New insights from simple experiments with plasticine. *Geology*, 10: 611-616.

Wilson, M. 1989. *Igneous Petrogenesis*. Unwin Hyman, London.

Received 16 July 2010

Accepted 23 August 2010